UCRL-JRNL-200144

Elucidating the Role of Many-Body Forces in Liquid Water. I. Simulations of Water Clusters on the VRT (ASP-W) Potential Surfaces

N. Goldman, R. J. Saykally

October 6, 2003

Journal of Chemical Physics

Elucidating the Role of Many-Body Forces in Liquid Water. I. Simulations of Water Clusters on the VRT(ASP-W) Potential Surfaces

UCRL-JP-200144

Nir Goldman[†,*] and R. J. Saykally[‡]

Abstract

We test the new VRT(ASP-W)II and VRT(ASP-W)III potentials by employing Diffusion Quantum Monte Carlo simulations to calculate the vibrational ground-state properties of water clusters. These potentials are fits of the highly detailed ASP-W *ab initio* potential to $(D_2O)_2$ microwave and far-IR data, and along with the SAPT5s potentials, are the most accurate water dimer potential surfaces in the literature. The results from VRT(ASP-W)II and III are compared to those from the original ASP-W potential, the SAPT5s family of potentials, and several bulk water potentials. Only VRT(ASP-W)III and the spectroscopically "tuned" SAPT5st (with N-body induction included) accurately reproduce the vibrational ground-state structures of water clusters up to the hexamer. Finally, the importance of many-body induction and three-body

[†]Lawrence Livermore National Laboratory, Chemistry and Materials Science Directorate, L-268, Livermore, California 94551

[*]Corresponding author. Email: goldman14@llnl.gov.

[‡]Department of Chemistry, University of California, Berkeley, California 94720-1416

dispersion are examined, and it is shown that the latter can have significant effects on water cluster properties despite its small magnitude.

1 Introduction

Given the recent determinations of accurate and highly detailed 2-body potentials for water from the spectroscopic data available for the water dimer [1–4], in conjunction with high level *ab initio* results [5–7], we are presented with an opportunity to explore the intricacies of intermolecular forces governing the liquid and solid phases of water. In a recent paper, Hodges et al. calculate the total *ab initio* interaction energies for the water trimer, tetramer and pentamer and dissect them into their respective N-body components [8]. The results show that the 2-body forces comprise ca. 75% of the total energy, the 3-body terms ca. 20%, and the 4–5-body terms the remaining 5%. In a more detailed paper, Ojäme and Hermansson performed a similar analysis of many-body forces operative in chains of water molecules up to the heptamer, in ring structures up to the pentamer, and in a tetrahedral pentamer [9]. These calculations, performed at the MP2 level, yield some striking insights. In both the water heptamer chain and the pentamer ring structure, they find that 2-body forces account for over 80% of the total interaction energy, and that two- and three-body terms together account for over 99%. In the tetrahedral pentamer, which closely resembles the average liquid and normal ice structures, they find that the two-body energy constitutes over 87% of the total interaction energy, and the two- and three-body terms together comprise ca. 99.6%. In all cases, the total energies of larger clusters are rapidly converging and are essentially fully converged by accounting for only the two- and three-body terms. Hence, description of the pairwise interaction

appears to be of paramount importance for constructing a complete molecular (i. e., non-empirical) description of the liquid.

Two of the most accurate water dimer potentials obtained to date are the recently determined VRT(ASP-W)II and III water dimer intermolecular potential energy surface (IPS) [2]. These are the second and third fittings, respectively, of Millot and Stone's ASP-W *ab initio* potential [10] to $(D_2O)_2$ intermolecular vibration-rotation (VRT) tunneling transitions. The dimer tunneling splittings from hydrogen bond rearrangements and the intermolecular vibrational frequencies provide a highly sensitive probe of the complex water intermolecular potential energy surface (IPS) [11], and such measurements have been made extensively by our laboratory [12–14]. The ASP-W potential has 72 parameters, corresponding to electrostatic interactions, two-body exchange-repulsion, two-body dispersion, and many-body induction, but it was found previously that accurate fits to the data could be produced by fitting 4-6 of the 22 exchange-repulsion parameters [15]. Thus, the VRT(ASP-W)II IPS was created by fitting 4 of the exchange-repulsion parameters in ASP-W [10] to 25 experimentally derived $(D_2O)_2$ microwave and far-IR transitions, and the VRT(ASP-W)III potential was generated by fitting 6 of the exchange-repulsion parameters to an additional 5 far-IR vibrational band origins. VRT(ASP-W)II and III constitute substantial improvements over the original VRT(ASP-W) potential [2], although van der Avoird and co-workers have obtained one of comparable quality for the $(H_2O)_2$ isotopomer by "tuning" an *ab initio* potential derived from symmetry adapted perturbation theory (SAPT) [3], discussed below.

Diffusion quantum Monte Carlo (DMC, discussed below) calculations on the ASP-W IPS have shown that induction is by far the most important many-body term in the

total cluster interaction energy [16], which was also confirmed by *ab initio* calculations [17]. Considering the fact that the VRT(ASP-W) dimer potential explicitly contains many-body induction in the form of electric multipoles and a tensorial polarizability, this IPS may actually be closer to a "universal" model for water than one would anticipate. However, it is important to note that [8] and [9] study relatively small systems and thus neglect long-range correlations which are present within the liquid (cf., ref. [18]) . Hence, it is possible that the total interaction energy of liquid water may not be as rapidly convergent as that for clusters. It is the goal of this and a forthcoming paper to explore the details of these subtle correlations that are present in the liquid.

Given its accuracy for describing the dimer, the next logical step is to test the VRT(ASP-W) IPS family of spectroscopic potentials in quantum simulations of higher clusters. Much spectroscopic data exist for larger clusters, particularly ground-state properties of up to hexamer [19–24]. We can thus simulate larger clusters with these potentials and compare results to the data in order to further test the validity of our IPS models. Diffusion quantum Monte Carlo is a useful simulation technique for such purposes [25–30]. It is a fully quantum mechanical technique with a computational cost that scales favorably with cluster size and potential complexity. Furthermore, it is an excellent complement to *ab initio* calculations because directly observable vibrationally averaged properties are calculated, rather than just the (unobservable) equilibrium properties. Quack and Suhm have utilized DMC extensively in similar studies of $(HF)_n$ clusters [31–35] and have determined highly accurate potentials for HF aggregates.

The starting point of a DMC simulation is the time-dependent Schrödinger equa-

tion, which is rewritten in imaginary time and thus becomes isomorphic with the diffusion equation. Consequently, the eigenstate of interest can be simulated via random diffusion. The original formulation for DMC was developed by J. Anderson in order to study one- to four-electron systems [36, 37]. There are a number of articles reviewing DMC, and thus the technique will not be discussed herein. For further information, the reader is in particular directed to the excellent review article by Suhm and Watts [38]. Further specific information on DMC simulations of water clusters can be found in a series of papers by Gregory and Clary [25–29]. All of the IPS used in the cluster calculations herein use a "frozen monomer" approximation, in which intramolecular degrees of freedom are not explicitly included in the calculation. Such IPS will be henceforth referred to as rigid potentials. Since inter-molecular degrees of freedom are treated separately from intra-molecular vibrations, and are of a lower frequency, a larger time step can be used in the rigid body simulations. A simple method for treating monomers as rigid-bodies has been developed by Buch and others [39, 40], called RBDMC, and again the reader is referred to the those references for further information. There are limitations to Diffusion quantum Monte Carlo, however, primarily in its inability to calculate excited states. Considerable recent progress has been made in that area and the reader is directed to the listed references for details [26, 41, 42]. Nonetheless, current excited state DMC algorithms are complicated and difficult to implement, and their ability to simulate excited states is still being assessed. Therefore, we restrict our present interests to the nodeless ground-state.

In the following, we present vibrational ground-state DMC results for the water dimer through hexamer for a variety of different potential energy surfaces. Results

from VRT(ASP-W)III are compared to those from experiment and ASP-NB (N-Body) created by Gregory and Clary [28] by adding an approximate form for 3-body dispersion (Axilrod-Teller-Muto triple-dipole interaction, discussed below) to the original ASP-W potential of Millot and Stone [10]. Comparisons between VRT(ASP-W)II and III are made in order to assess the effects of our fits on vibrational ground-states of water clusters greater than the dimer. Due to the high level of accuracy attained for the dimer [6] and trimer [7], simulation results from the SAPT5s family are presented as well. Additional comparisons are made to SPC/E [43], and PSPC [44], to investigate how the properties of these bulk water potentials differ from those of the gas phase models in terms of cluster simulations. Based on comparison to MP2 results from Reference [28] and to experimental results, the effectiveness of including induction as the only many-body force is evaluated. The effects of three-body dispersion in DMC simulations is then quantified.

2 Ground-state properties of water clusters: comparison to experiments

In all RBDMC simulations performed here, a population of 1000 walkers was used, and these comprised an equilibration stage followed by a propagation stage over which properties were averaged. For the dimer, trimer and tetramer, equilibrium periods of 2000 time steps of 40 a. u. were used, while those for the pentamer and hexamer were longer, consisting of 6000 time steps at 40 a. u. This was necessary due to the high dimensionality of the IPS used in our simulations and the existence of numerous local minima and potential barriers. The ground-state eigenvalues were obtained

by averaging E_R over the entire propagation stage of 15,000 to 20,000 time steps of magnitude 20 a. u., and histograms of configurations were used to calculate the inertial tensor, and hence, the moments of inertia and rotational constants.

In order to completely characterize the potential energy surfaces, searches for local minima were performed using the eigenvector following method, available in the Orient 4.4 program [45]. Starting geometries were taken from RBDMC simulations or were generated randomly. An exhaustive search for minima was too time consuming, considering the large number of local minima Gregory and Clary found for the pentamer and hexamer [28], so searches for structures already identified by Gregory and Clary with the ASP-NB IPS (discussed below) that were deemed important were performed instead. To distinguish these structures from vibrational ground-state structures, we labeled the equilibrium structures determined by Orient 4.4 as **ES,** and the vibrational ground-state structures determined from DMC as **VGS**.

When examining dissociation energies D_0 of local minima structures, the constraint suggested by Gregory and Clary was to keep the simulation in the local minimum of interest [28]. In such a quantum simulation, collapse to a lower energy structure is usually caused by a single walker moving out of the given minimum and hence causing the entire walker population to drift out of the well. To prevent this, one can simply delete any walker that is of lower energy than D_e of the local minimum being studied, forcing the simulation to remain within that particular local minimum.

Comparisons are made to the D_e and D_0 values found by Gregory and Clary, in [28], both from RBDMC and *ab initio* calculations, the former performed with the ASP-NB potential. This potential was derived by taking the ASP-W potential [10], which includes many-body induction, and adding 3-body dispersion via a simple

Axilrod-Teller-Muto (ATM) triple-dipole term [46, 47]. Their *ab initio* calculations were performed using second-order Møller–Plesset (MP2) perturbation theory and a double-ζ plus polarization basis, and they computed D_0 values for clusters up to and including the tetramer from the MP2 harmonic frequencies.

RBDMC calculations were performed on the original ASP-W and VRT(ASP-W)II and III. VRT(ASP-W)III emerged as the best of these models, both because it was fit to the largest set of experimental data, and via comparison of ground-state structures of the dimer through hexamer. In terms of $(H_2O)_2$, VRT(ASP-W)II and III are quite similar, as evidenced by the computed $(H_2O)_2$ properties calculated. However, as will be shown below, fitting VRT(ASP-W)III to this slightly larger parameter and data set produced an IPS that is not only a better dimer potential, but one that is also a better model for larger clusters.

Calculations have also been performed on the SAPT family of potentials for the water dimer, as mentioned above. The SAPT5s *ab initio* pair potential was developed a few years ago and was shown to have near-spectroscopic accuracy [3, 4, 6], but it is strictly a pair potential and cannot be used to accurately simulate clusters larger than the dimer.

In a more recent publication [7], Mas et al. extended the SAPT5s formalism to include three-body forces by performing supermolecular SCF and three-body SAPT calculations for 7533 trimer geometries. The nonadditive energies from these calculations were then fit to an analytic formula motivated by the SAPT analysis and containing representations of short-range exchange and damped induction contributions. This form of three-body exchange and induction was then combined with the SAPT5s dimer potential to form the SAPT5s+3B IPS, which was tested extensively

for $(H_2O)_3$ and $(D_2O)_3$ equilibrium structure and energetics, and used to simulate the liquid [48]. To the best of our knowledge, SAPT5s+3B is the only existing 12D (i. e., including all intermolecular coordinates, with frozen monomers) non-additive *ab initio* potential for the water trimer with explicit three-body exchange terms. However, SAPT5s+3B by itself omits a description of the N>3-body forces acting within clusters, viz. N>3-body induction, which are the largest N-body forces.

In order to simulate clusters larger than trimer, we included N-body induction in SAPT5s+3B in a similar fashion to Mas et al. [48], viz. by calculating the N-body induction from VRT(ASP-W)III and subtracting off the total 3-body and total 2-body induction. Hence, the 2-body and 3-body induction used in these simulations was performed on the SAPT5s+3B potential, and the N>3-body induction was calculated on VRT(ASP-W)III. We called this N-body form of the potential, SAPT5s+NB(ASP). For further clarification, the dimer simulations were performed on SAPT5s, the trimer on SAPT5s+3B, and the tetramer through hexamer on SAPT5s+NB(ASP). Unfortunately, the repeated calculation of iterated induction via VRT(ASP-W)III made all simulations with SAPT very costly. Hence, calculations were performed for H_2O clusters only. Also, the 3-body forces in the SAPT code were not compatible with the Orient 4.4 software. Hence, the only equilibrium data given herein are those already reported for the dimer [6] and trimer [7]. As stated above, there also exists a fitted "tuned" form of SAPT5s called SAPT5st, which has an even higher degree of spectroscopic accuracy for $(H_2O)_2$. However, since the recent publications of Mas et al. [7, 48] deal exclusively with the un-tuned SAPT5s potential, and due to the high computational cost of including N-body induction, we decided to limit the RBDMC simulations with SAPT5st to the pentamer and hexamer. Both of these clusters are

crucial for determining the accuracy of the IPS, and SAPT5s+NB(ASP) has proven accurate only up through the pentamer is accurate for both the pentamer and hexamer (Section 2.4). The N-body form of SAPT5st was called SAPT5s+NB(ASP-T), in order to readily distinguish it from the un-tuned SAPT5s IPS.

Simulations were also performed on the SPC/E [43] and PSPC [44] models for liquid water. SPC/E is a popular and reasonably good model for room temperature water at normal density [49]. PSPC is one of several polarizable potentials with the same pairwise functional form as SPC/E (cf., [50]). Its model for polarizability is fairly crude, since it ascribes atomic polarizabilities to the oxygen and hydrogens of the water monomer, rather than allowing for anisotropy via a second rank polarizability tensor for each monomer. It is not as accurate as SPC/E in terms of the total liquid dipole moment and diffusion constant at standard thermodynamic conditions, but it does accurately reproduce the gas phase water dimer dipole moment and is able to produce reasonable radial distribution functions for the liquid that clearly reflect tetrahedral structure. Consequently, because it contains induction terms, it should act as a good "transition" potential in that it would serve as a reasonable model for bridging the gas and bulk phases. In particular, we thought it would be interesting to see at what cluster size, if any, SPC/E, PSPC and our gas-phase cluster models begin to exhibit the same structural properties, and perhaps indicate when gas-phase clusters might truly begin to mimic the bulk.

2.1 $(H_2O)_2$

The water dimer structure is shown in Figure 1, the values of D_e and D_0 are shown in Table 1, and the rotational constants are given in Table 2.

It is important to note in Table 1 that the MP2 harmonic D_0 energy is much higher than most of the other predictions (excluding PSPC), clearly evidencing the large anharmonicity of the dimer vibrations. The rotational constants from VRT(ASP-W)II and III are both within a few percent of experimental values. The published results for SAPT5s yield a value for A that is ca. 9% too small, but values for B and C that are very close to (within less than 1%) experimental values. SPC/E yields B and C rotational constants that are much too high due to the fact that the $\langle R_{OO} \rangle$ value that it predicts (2.82 Å) is much shorter than the experimental dimer value (2.99 Å). PSPC gives an $\langle R_{OO} \rangle$ value (2.99 Å) and rotational constants that compare well to experiments. However, it gives a value of D_0 that is significantly higher than all other potentials (ca. 17% above that from VRT(ASP-W)III), including the MP2 surface. Also, both SPC/E and PSPC have values of D_e that are vastly lower than all other IPS that were tested.

2.2 $(H_2O)_3$

The global minimum in all potentials tested is the (uud) structure (Figure 2) wherein two of the free hydrogens point up from the [OOO] plane while the third points downward. The first local minimum in all potentials is the (uuu) structure (Fig. 2), wherein all three free hydrogens point upward form the [OOO] plane. The detailed structure of the global minimum is consistent with experimental results, as reviewed recently by Keutsch et al. [51].

The values for D_e and D_0 are shown in Table 3. VRT(ASP-W)II continues to compare well to version III, yielding values of D_e and D_0 that are all within a few percent. The values of D_e and D_0 for SAPT5s+3B are 3% and 1.5% lower, respec-

tively, than those for VRT(ASP-W)III. It is interesting to note that the value of D_0 for SPC/E is significantly higher than those of the other potentials, whereas it was instead much lower for the dimer. This is most likely due to the highly non-linear hydrogen bonding geometry obtained in the trimer. D_0 for PSPC is now ca. 27% higher than that of VRT(ASP-W)III, indicating that it fails to model some of the cooperative effects present in the VRT(ASP-W)III trimer, at least in this geometry.

Rotational constants for $(H_2O)_3$ and $(D_2O)_3$ for all potentials are shown in Table 4. Experimental rotational constants measured for $(D_2O)_3$ confirm that the (uud) structure is the VGS. As expected, the rotational constants of the VGS correspond to an oblate top (A = B > C). The calculated rotational constants of the VRT(ASP-W)III D_2O trimer correspond reasonably well, although the A rotational constant is ca. 15% too high, causing the (uud) structure to be distorted to that of an asymmetric top. Interestingly, the SAPT5s+3B potential yielded rotational constants that are nearly identical to those from VRT(ASP-W)III. The ASP-NB IPS is able to more closely predict the oblate top as a ground state structure, although the calculated values of A and B are ca. 20% too high. This is surprising, considering that ASP-NB was not fit to experimental data and the included three-body dispersion forces are generally considered small enough to neglect [8]. However, it should be noted that the B rotational constant of VRT(ASP-W)III is much closer to the actual experimental result.

Finally, effort was made to constrain the DMC simulation into the (uuu) potential well. As shown in Table 3, all simulations eventually collapsed into the (uud) ground-state. This is consistent with the findings of Gregory and Clary [28], and is likely due to the low potential barrier for flipping of the down (d) hydrogen.

2.3 $(H_2O)_4$

It is well-established [1, 28] that the VGS for the tetramer is the cyclic (udud) structure, shown in Figure 3(a). However, other stable low energy structures are possible, as demonstrated by a search for local minima on the IPS. Figure 3, (b) – (e) show the lowest-lying structures found by us and by Gregory and Clary [28]. Excluding SPC/E, all of the IPS tested here showed the (udud) structure as the global minimum, consistent with most previous work. On the VRT(ASP-W)III IPS, the only additional minima found were the cyclic (uudd) and (uuud) structures.

Results of Orient 4.4 and RBDMC calculations are shown in Tables 5. As stated in the Introduction, the SAPT5s code was not compatible with the Orient4.4 software; hence, the local minima of SAPT5s+NB(ASP) were not explored. Excluding SPC/E and PSPC, all of the potentials show good agreement with the MP2 D_e and D_0 results, and D_0 from SAPT5s+NB(ASP) was 6.5% lower relative to VRT(ASP-W)III. As Gregory and Clary point out, for both (uudd) and (uuud) there are two cis- and two trans-type interactions, which explains why these structures are consistently similar in energy. In the (udud) structure, there are four trans-type interactions, which explains why it is lower in energy. The SPC/E result is particularly distant from other calculations, with a D_0 that is ca. 40% higher and a VGS of (uudd). The high VGS dissociation energy results from the fact the the tetramer also has highly non-linear hydrogen bonds, not well described by this bulk liquid model. PSPC predicts the (udud) structure as the VGS, but has a D_0 ca. 34% higher than that of VRT(ASP-W)II or III.

We attempted to calculate D_0 for the (uudd) and (uuud) structures on the VRT(ASP-W)III surface and found that they collapsed to the more stable (udud) structure. This

is consistent with Gregory and Clary's findings, where they point out that they expect the above to happen since the flipping of a hydrogen should be very facile. Our inability to locate a cage minimum is also consistent with their results, since they found the cage structure to collapse to (udud) for both ASP-NB and MP2. However, they were able to locate the C_S ES on both surfaces, whereas we could not find this structure on VRT(ASP-W)III.

Vibrationally averaged rotational constants for all global minima are shown in Table 6, and comparison is made to experimental results for $(D_2O)_4$. Rotational constants for $(H_2O)_4$ have not yet been measured at the time of this publication. Interestingly, the SAPT potential once again yields rotational constants that are very similar to those from VRT(ASP-W)III, with the value of B deviating the most, but by only ca. 4%. In terms of $(D_2O)_4$, ASP-NB results are quite close to the experimental properties of an oblate top. VRT(ASP-W)III performs very well, with the average of A and B differing from experiment by less than 10%. Again, calculations were not performed on SAPT5s+NB(ASP) for $(D_2O)_4$ due to the high cost of the simulation.

2.4 $(H_2O)_5$

There have been a number of structural studies of the water pentamer using various empirical potentials, as discussed by Gregory and Clary [28]. Most of these studies predict a low-energy cyclic structure, although other structures are also found to be the global minimum, and all studies predict several structures of similar energy. The general belief that the cyclic structure is the global minimum initiated a number of studies on this particular structure, which was characterized experimentally by Liu et al [20].

Contrasting the cases of the trimer and tetramer, several local minima were found on the VRT(ASP-W)III potential. Our energy minimization searches were limited to the three lowest lying ES, shown in Figure 4. The cage (6) structure is differentiated from the cage (7) structure in that it contains a network of 6 hydrogen bonds instead of 7. It is lower in energy because, although it has fewer hydrogen bonds, the ES is not as contracted and thus can achieve more nearly linear hydrogen bonding, very close to the ideal hydrogen bond geometry. The envelope is made up of a (udud) tetramer structure with an additional monomer hanging off to one side and out of the [OOOO] plane.

Investigation of the global minima of the pentamer potential energy surfaces, shown in Table 7, proved to be very interesting, as the potential models predict a variety of different VGS. The correct cyclic pentamer VGS was predicted by MP2 surface, VRT(ASP-W)III, SAPT5s+NB(ASP) and SAPT5s+NB(ASP-T), and these four potentials contain minimal differences in terms of the ground0-state and equilibrium properties. The predicted values of D_e from the MP2 calculations and VRT(ASP-W)III are within 60 cm^{-1} of each other, which is remarkably close. The value of D_0 from SAPT5s+NB(ASP) deviates from that of VRT(ASP-W)III by +6.2%, and that from SAPT5s+NB(ASP-T) by +3.8%. Again, our DMC simulations of the "tuned" SAPT5s+NB(ASP-T) were limited to pentamer and hexamer, due to the high computational cost of including N-body induction in the simulation, and because recent trimer and liquid studies of the IPS deal exclusively with the un-tuned form of the potential.

ASP-NB, VRT(ASP-W)II, PSPC and SPC/E all predict a wide variety of vibrational ground-state structures, other than the cyclic structure. ASP-NB predicts the

cage(6) structure for the global minimum for both D_e and D_0, which is somewhat surprising, considering how remarkably well this IPS performed for the dimer, trimer, and tetramer. Comparison of VRT(ASP-W)II to VRT(ASP-W)III is also interesting, since VRT(ASP-W)II has a global minimum of the cyclic structure but predicts the envelope as the vibrationally averaged ground-state. Noting that an equivalent basis set was used for each fit, this demonstrates the extreme sensitivity of the IPS to subtle details. The PSPC potential predicts the cyclic structure as the VGS, although once again the value of D_0 is considerably higher than all of the other surfaces, ca. 34% in this case. SPC/E predicts the tetrahedral-like structure for the VGS, as shown in Figure 5. Given its tetrahedral parametrization, this is not particularly surprising. The structure shown is taken from a snapshot of a walker at the very end of an RB-DMC simulation. The fact that the pentamer accommodates this preferred structure, with linear hydrogen bonds, undoubtedly accounts for the large drop in D_0 in going from the tetramer to the pentamer.

Energetics of pentamer structures are summarized in Table 8, excluding those from PSPC and SPC/E, which again were not tested as extensively due to their inaccuracy in predictions of pentamer ground-state properties, and SAPT5s+NB(ASP) and SAPT5s+NB(ASP-T), due to their incompatibility with Orient 4.4. Comparison of the MP2 results for the envelope and cage(6) to the other surfaces shows that the MP2 values of D_e are a small but significant amount higher – 5% higher and 3% higher respectively, compared to VRT(ASP-W)III. Such small differences can prove significant, as highlighted by comparison of results from VRT(ASP-W)II and III; their values for the ground-state D_e and D_0 are within 1% of each other, and yet each predicts different ground-state structures.

Vibrationally averaged ground-state rotational constants for $(H_2O)_5$ are shown in Table 9, and comparison is made to experimental results for $(D_2O)_5$. (Again, rotational constants for $(H_2O)_5$ have not been measured at the time of this publication.). Also, the rotational constants from SAPT5s-NB(ASP) and SAPT5s-NB(ASP-T) are fairly close (within 10%) to those from VRT(ASP-W)III. The cyclic structure rotational constants of ASP-NB were reported by Gregory and Clary, and although they do not predict it as the VGS, they do predict rotational constants from simulations constrained to the cyclic structure potential minimum that are quite close to experiment. VRT(ASP-W)III also does reasonably well, as the average of A and B is within 15% of experimental values.

2.5 $(H_2O)_6$

There is significant theoretical interest in the hexamer, since it is the first experimentally characterized water cluster VGS that has a 3D arrangement of monomer center of masses. Experimental results [21] have indicated that the ground-state structure is most likely the cage, shown in Figure 6. Indeed, because of this, it has been proposed as a prototype for analyzing hydrogen bonding in ice [21].

As with the pentamer, it is well-known that there is a large number of nearly isoenergetic ES near the actual global minimum, the most relevant of which are shown in Figure 6. The global minimum (equilibrium structure) on all potential surfaces examined here is the prism structure, shown in part (a). Table 11 shows that for all potentials, excluding the MP2 surface, the prism is significantly lower in energy than all other structures, with the cage structure being the closest to it. In the case of VRT(ASP-W)II and III, the prism structure is energetically even further from

the cage than on the ASP-NB surface. VRT(ASP-W)II and III agree more closely with the MP2 surface in that they also predict the cyclic and book structures as the next two structures in terms of energetic ordering. ASP-NB predicts that the cyclic structure is higher in energy than the cage, most likely a flaw in the potential since high level *ab initio* calculations predict the cyclic structure to be close to the prism and cage [52]. This is consistent with our findings for VRT(ASP-W)II and III.

RBDMC vibrationally averaged ground-state properties for all IPS are shown in Table 10. There are some important observations to make about the predicted VGS. VRT(ASP-W)II predicts the prism as the VGS, whereas VRT(ASP-W)III correctly predicts the cage structure to be lowest in D_0 energy and the prism to be the next highest. Once again, this is surprising considering how similar the two IPS were thought to be, and it again testifies to the "correctness" of the VRT(ASP-W)III IPS. SAPT5s+NB(ASP) yields a value for D_0 that is once again within ca. 6.5% of that from VRT(ASP-W)III, but incorrectly predicts the book as the VGS. Efforts were made to constrain the simulations on SAPT5s+NB(ASP) to the cage structure local minimum by using the cage configuration from VRT(ASP-W)III determined by Orient4.4 as the starting configuration for the walkers. However, each attempt as such resulted in a prism structure with a value of D_0 of -10713 cm^{-1}. This seems to indicate that the SAPT5s+NB(ASP) surface incorrectly predicts the ground-state structures of $(H_2O)_6$. However, simulations with the "tuned" SAPT5s+NB(ASP-T) yielded the correct VGS of the cage structure, and a value of D_0 within ca. +7% of that for VRT(ASP-W)III. Once again, this is very surprising considering considering the similar high degree of accuracy of both the SAPT5s and SAPT5s-T IPS families for cluster VGS up through the pentamer. The results for the hexamer once again

illustrate the subtle but significant effect the fitting of an IPS to spectroscopic data can have, and thus highlights the importance of continuing such efforts.

Also interesting to examine are the two structures predicted by the "bulk" potentials, PSPC and SPC/E. PSPC deviates significantly from experimental results by predicting a book VGS that is roughly 40% higher in energy than all other ground-state predictions. SPC/E exhibits a D_0 closer in energy to the gas phase IPS, but in keeping with its propensity for tetrahedral structure, it predicts a "bird-like" VGS, shown in Figure 7. This structure is once again taken from a snapshot of a random walker during an RBDMC simulation. It resembles a distorted cyclic tetramer with the next two monomers up top sticking in and out of the [OOOO] plane. Hence, the bird has a mirror image plane that is defined by [OOOO]. Due to the effectiveness of SPC/E surface in simulating the bulk at standard conditions, as discussed below, this structure can be seen as a snapshot of what a hexamer instantaneously formed in the liquid would most probably look like.

The ground-state rotational constants for each potential are listed in Table 12. VRT(ASP-W)III, SAPT5s+NB(ASP-T) and ASP-NB are all in good agreement with the listed experimental results for $(H_2O)_6$.

2.6 Discussion

The vibrationally averaged nearest neighbor O–O distances for H_2O ground-state clusters calculated on several of the potentials are shown in Figure 8. As the figure shows, VRT(ASP-W)III performs very well as a model for higher order clusters. Upon examination of results for the pentamer and hexamer, it is clear that it represents a substantial improvement over VRT(ASP-W)II. As we have noted, this is surprising,

considering that VRT(ASP-W)III represents a relatively minor refinement of version II in terms of dimer properties. However, this subtle refinement has major global consequences, since VRT(ASP-W)III is a much better model for the larger clusters. Hence, continued fitting of ASP-W or other IPS to larger spectroscopic data sets seems to be a worthwhile pursuit. Moreover, although SAPT5s+NB(ASP) describes clusters up through the pentamer quite well, "tuning" of an IPS to experimental data is clearly important since VRT(ASP-W)III and SAPT5s+NB(ASP-T) are the best models currently in existence for gas-phase clusters. The fact that the only many-body force present in VRT(ASP-W)III is induction supports the assertion that for gas-phase cluster calculations it seems reasonable to neglect all other many-body contributions (i. e, dispersion, exchange); hence, the computational cost of including 3-body exchange in VRT(ASP-W)III does not seem worthwhile. In addition, there does not exist a computationally cheap method for including 3-body exchange with VRT(ASP-W)III. In SAPT5s+3B, the three-body induction and exchange parameters were fit to the entire SCF non-additive energy. Hence, due to correlations between parameters, one cannot simply insert the non-additive exchange terms into a DMC simulation with VRT(ASP-W)III, and would require a technique similar to what was used to calculate the N>3-body dispersion on the SAPT5s+3B potential surface.

In order to ascertain how VRT(ASP-W)III might perform in bulk simulations, it is instructive to compare VGS calculations between it, SPC/E and PSPC. SPC/E is the water model most widely in use and arguably the most accurate. It predicts a very accurate value for water surface tension at room temperature and above [49]. The surface tension is dependent upon the average value of the components of the pressure tensor, which is itself dependent upon the radial intermolecular force acting

upon each monomer. As a result, surface tension can be viewed as a measure of the average force field experienced by the monomers.

In light of the above statement, RBDMC results from SPC/E most likely represent the highest probability structures for clusters that may form instantaneously in the bulk. As is shown by examining Figures 5 and 7, in the SPC/E bulk, monomers have a strong tendency to form structures more closely resembling tetrahedrons. The fact that these VGS differ so vastly from both experimental results and from those produced by VRT(ASP-W)III indicates that $(H_2O)_6$ may not be the best prototype for investigating bulk water hydrogen bonding, as has been proposed in the literature [21]. Indeed, although $(H_2O)_6$ may have a value for $\langle R_{OO} \rangle$ and an O–H$\cdots$O bond angle that is close to bulk values, it clearly lacks the signature tetrahedral structure present in the bulk. Hence, it appears that the continued experimental investigation of clusters larger than the hexamer is important in order to further elucidate structural details of the hydrogen bond network of the liquid and solid forms of water.

In addition, it is very interesting that for the pentamer and hexamer, SPC/E has a VGS energy that is lower than those from VRT(ASP-W)III, by 53 cm^{-1} and 1180 cm^{-1}, respectively. Assuming this trend continues, and that for N>5-body clusters, SPC/E generally produces a lower D_0, this implies that VRT(ASP-W)III is still missing long-range attractive correlations that are important for correctly simulating the structure of the bulk. This important implication will be investigated more thoroughly in a forthcoming paper (II).

Our investigations of PSPC are interesting but not quite as enlightening. The model is able to predict reasonably accurate ground-state structures, at least up to the pentamer. However, in terms of its energetics, it serves as a poor model in that

it predicts values of D_0 that were consistently much higher than those of our IPS as well as the MP2 surface. This is most likely due to simplistic representation of molecular polarizabilities in terms of the constituent atomic ones. As a result, the model may not properly take into account cooperativity effects within clusters and thus underestimates the effects of induction. The fact that despite this, or maybe because of it, PSPC serves as a reasonable structural model for the liquid makes the idea of performing liquid simulations with VRT(ASP-W)III intriguing.

3 The role of three-body dispersion

Considering the relatively high quality of the ASP-NB potential, it is of interest to perform a thorough analysis of the effects of the approximate form of the triple-dipole dispersion on energetic global minima and vibrational ground-state properties of water clusters. Although the effects are most likely quite small, inclusion of this three-body dispersion term greatly improved the performance of the ASP-W potential, as shown before by Gregory and Clary [28].

The simple Axilrod-Teller-Muto (ATM) expression for triple dipole dispersion is a simple isotropic approximation to the true tensorial form, detailed in Refs. [46] and [47]. Its effect on ASP-W will be quantified through comparison of RBDMC and Orient4.4 simulation results for the dimer through hexamer. Finally, some conclusions will be drawn as to its relevance to VRT(ASP-W)III.

3.1 Dispersion effects in ASP-W clusters

In order to quantify the dispersion effects in ASP-NB, the dimer through hexamer were simulated with ASP-W with converged induction. As mentioned in Section 2, ASP-NB differs from ASP-W only in that it contains the ATM approximation for 3-body dispersion. The effects on D_e are shown in Table 13.

For the most part, the three-body dispersion effects on the interaction energy seem to be minimal, and fractional changes are on the order of 1% and less. The single structure that experiences significant energetic change is the C_S tetramer, which is over 12% higher for ASP-W. This is undoubtedly due to the fact that the four possible triplets in the structure form obtuse triangles which have attractive three-body dispersion energies. The changes induced in the pentamer and hexamer are subtle, but significant as well. For the ASP-W pentamer, the energetic ordering has changed from the cage(6) to the envelope as the global minimum, followed by the cyclic structure, cage(6) and then cage(7). The reordering of the minima is possible because the minima all lie quite close to each other, so slight alterations of D_e can have significant effects. The changes for the hexamer are much less dramatic – the main feature to note is that the prism structure experiences attractive dispersion whereas the cage structure experiences a three-body repulsion. This causes the ASP-W structures to have a significantly larger energetic gap of 373 cm^{-1} vs. 21 cm^{-1} for ASP-NB.

The results for the VGS for the trimer through hexamer are shown in Table 14, and the corresponding rotational constants in Table 15. As Table 14 indicates, the overall effect of the dispersion term on the VGS energy is quite small – at most a couple of percent, in the case of $(H_2O)_5$. Table 15 shows that the effect on ground-state

structural properties is much stronger. Structures for $(D_2O)_3$, $(D_2O)_4$ and $(D_2O)_5$ were all determined experimentally to be cyclic, corresponding to oblate tops. ASP-W consistently overestimates the A rotational constant, and in the case of $(D_2O)_5$, the envelope emerges as the VGS. Due to the larger energy gaps between the prism and cage structures, the ASP-W $(H_2O)_6$ VGS is the prism. We have not attempted to reproduce Gregory and Clary's results for ASP-NB, but according to reference [28], it does an excellent job of ground-state structural prediction. It yields perfect oblate tops for $(D_2O)_3$, $(D_2O)_4$ and $(D_2O)_5$, and rotational constants for the $(H_2O)_6$ cage that are very close to experimental results. Nonetheless, the results seem somewhat unreasonable considering the small percent of the interaction energy that corresponds to dispersion. Certainly it seems plausible that the addition of dispersion may cause $(D_2O)_3$ and $(D_2O)_4$ to become more oblate, and thus for $(D_2O)_5$ and $(D_2O)_6$ to match experiments more closely , but the values of A obtained for the ASP-W $(D_2O)_3$ and $(D_2O)_4$ clusters are close to 20% greater than those reported in [28]. These changes appear to be too great to be able to be corrected by Axilrod-Teller dispersion. Verifying their calculations is not worthwhile at this point, but it seems that those results should be viewed with caution.

3.2 Discussion

Despite the fact that three-body dispersion may have resulted in significant changes in some of the ASP-W cluster properties, it does not seem worthwhile to quantify the effects it would have on VRT(ASP-W)III. The potential minima in VRT(ASP-W)III are not spaced as close together as those in ASP-W, so it is not expected that ATM three-body dispersion could cause a reordering of energetic structures. For example,

for the VRT(ASP-W)III pentamer, the smallest energy difference in D_e is between envelope and cyclic structures, which are 205 cm^{-1} apart. This corresponds to ca. 1.55% of the value of D_e for the envelope, which according to Table 13 would be the very upper limit for the ATM effects.

It is important to note again that the ATM three-body dispersion is isotropic and consequently is less accurate than a tensorial representation of the triple dipole-interaction. The effect of using a more accurate triple-dipole dispersion term can be estimated if we view the tensorial interaction as the inclusion of additional degrees of freedom over an isotropic representation. Additional degrees of freedom would allow a water cluster to "relax" energetically more easily if a given interaction were repulsive, and they would allow the cluster to enhance the interaction if it were attractive. Thus, it follows that the the repulsive three-body interactions in such a tensorial representation would be smaller than those of the ATM approximation, and the attractive interactions would be larger. Hence, it is clear that further energetic reordering of local minima will take place, especially in clusters where the the local minima are nearly isoenergetic, such as with the pentamer, hexamer and larger clusters. Regardless, as stated in the Introduction, three-body exchange is significantly larger in magnitude than three-body dispersion. As a result, it is very important to include both types of forces in order to quantify the overall three-body effects on an IPS.

4 Discussion

We have developed [2] a new water dimer potential (VRT(ASP-W)III), from a fit to $(D_2O)_2$ spectroscopic data with induction as the only many-body body force included.

It predicts quite accurate ground-state properties for the water dimer through hexamer, and can thus serve as a good model for dynamics of larger clusters. This is an important step for the calculation of condensation properties, which requires accurate evaluation of the cluster free energy surface (for example, see [53]).

The improvement of VRT(ASP-W)III relative to version II is significant, and it is notable that the addition of just a few additional transitions greatly improved structural predictions for the pentamer and hexamer. The next test of VRT(ASP-W)III will be to employ it in actual liquid simulations. Whereas the proper inclusion of induction has been shown to be sufficient for simulations of clusters, there is a good chance that it is not sufficient to model the long range correlations present in the liquid. It is quite possible that other many-body effects, viz. dispersion and exchange may prove important for simulation of the bulk. This is examined in a forthcoming paper.

5 Acknowledgments

This work was supported by the Experimental Physical Chemistry Program of the National Science Foundation. The authors would like to thank Mac Brown for initial help with writing the DMC code, and Krzysztof Szalewicz and Robert Bukowski for use of their SAPT potential code and for many helpful discussions. They would also like to thank K.S. and R.B., as well as Anthony Stone for a critical review of the manuscript.

This work was performed under the auspices of the U.S. Department of Energy by the University of California, Lawrence Livermore National Laboratory under Contract No. W-7405-Eng-48.

References

[1] F. N. Keutsch and R. J. Saykally, Proc. Natl. Acad. Sci. U.S.A. **98**, 10533 (2001).

[2] N. Goldman, R. S. Fellers, M. G. Brown, L. B. Braly, C. J. Keoshian, C. Leforestier, and R. J. Saykally, J. Chem. Phys. **116**, 10148 (2002).

[3] G. C. Groenenboom, E. Mas, R. Bukowski, K. Szalewicz, P. E. S. Wormer, and A. van der Avoird, Phys. Rev. Lett. **84**, 4072 (2000).

[4] G. C. Groenenboom, P. E. S. Wormer, A. van der Avoird, E. Mas, R. Bukowski, and K. Szalewicz, J. Chem. Phys. **113**, 6702 (2000).

[5] C. Millot, J. C. Soetens, M. T. C. Martins-Costa, M. P. Hodges, and A. J. Stone, J. Phys. Chem. A **102**, 754 (1998).

[6] E. M. Mas, R. A. Bukowski, K. A. Szalewicz, G. C. Groenenboom, P. E. S. Wprmer, and A. van der Avoird, J. Chem. Phys. **113**, 6687 (2000).

[7] E. M. Mas, R. Bukowski, and K. Szalewicz, J. Chem. Phys. **118**, 4386 (2003).

[8] M. P. Hodges, A. J. Stone, and S. S. Xantheas, J. Phys. Chem. A **101**, 9163 (1997).

[9] L. Ojamäe and K. Hermansson, J. Phys. Chem. **98**, 4271 (1994).

[10] C. Millot and A. J. Stone, Mol. Phys. **77**, 439 (1992).

[11] R. J. Saykally and G. A. Blake, Science **259**, 1570 (1993).

[12] L. B. Braly, J. D. Cruzan, K. Liu, R. S. Fellers, and R. J. Saykally, J. Chem. Phys. **112**, 10293 (2000).

[13] L. B. Braly, K. Liu, M. G. Brown, F. N. Keutsch, R. S. Fellers, and R. J. Saykally, J. Chem. Phys. **112**, 10314 (2000).

[14] K. L. Busarow, R. C. Cohen, G. A. Blake, K. B. Laughlin, Y. T. Lee, and R. J. Saykally, J. Chem. Phys. **90**, 3937 (1989).

[15] R. S. Fellers, C. Leforestier, L. Braly, M. G. Brown, and R. J. Saykally, Science **284**, 945 (1999).

[16] J. K. Gregory and D. C. Clary, J. Chem. Phys. **103**, 8924 (1995).

[17] G. Chałasiński, M. M. Szczęśniak, P. Cieplak, and S. Scheiner, J. Chem. Phys. **94**, 2873 (1991).

[18] P. L. Geissler, C. D. Dellago, D. Chandler, J. Hutter, and M. Parrinello, Science **291**, 2121 (2001).

[19] K. Liu, J. G. Loeser, M. J. Elrod, B. C. Host, J. A. Rzepiela, and R. J. Saykally, J. Am. Chem. Soc. **116**, 3507 (1994).

[20] K. Liu, J. D. Cruzan, and R. J. Saykally, Science **271**, 929 (1996), and references therein.

[21] K. Liu, M. G. Brown, C. Carter, R. J. Saykally, J. K. Gregory, and D. C. Clary, Nature **381**, 501 (1996).

[22] K. Liu, M. G. Brown, J. D. Cruzan, and R. J. Saykally, Science **271**, 62 (1996).

[23] K. Liu, M. G. Brown, and R. J. Saykally, J. Phys. Chem. A **101**, 8995 (1997).

[24] N. Pugliano and R. J. Saykally, Science **257**, 1937 (1992).

[25] J. Gregory and D. C. Clary, Chem. Phys. Lett. **228**, 547 (1994).

[26] J. K. Gregory and D. C. Clary, J. Chem. Phys. **102**, 7817 (1995).

[27] J. Gregory and D. C. Clary, J. Chem. Phys. **103**, 8924 (1995).

[28] J. K. Gregory and D. C. Clary, J. Phys. Chem **100**, 18014 (1996).

[29] J. K. Gregory and D. C. Clary, J. Chem. Phys. **105**, 6626 (1996).

[30] J. K. Gregory, D. C. Clary, K. Liu, M. G. Brown, and R. J. Saykally, Science **275**, 814 (1997).

[31] M. Quack and M. A. Suhm, Mol. Phys. **69**, 79‘ (1990).

[32] M. Quack and M. A. Suhm, Chem. Phys. Lett. **183**, 187 (1991).

[33] M. Quack and M. A. Suhm, J. Chem. Phys. **95**, 28 (1991).

[34] W. Kloppera, M. Quack, and M. A. Suhm, J. Chem. Phys. **108**, 10096 (1998).

[35] M. Quack, R. Stohner, and M. A. Suhm, J. Mol. Struct. **599**, 381 (2001).

[36] J. B. Anderson, J. Chem. Phys. **63**, 1499 (1975).

[37] J. B. Anderson, J. Chem. Phys. **65**, 4121 (1976).

[38] M. A. Suhm and R. O. Watts, Phys. Rep. **204**, 293 (1991).

[39] V. Buch, J. Chem. Phys. **97**, 726 (1992).

[40] P. Sandler, J. O. Jung, M. M. Szczesniak, and V. Buch, J. Chem. Phys. **101**, 1378 (1994).

[41] M. W. Severson and V. Buch, J. Chem. Phys. **111**, 10866 (1999).

[42] D. Blume and K. B. Whaley, J. Chem. Phys. **112**, 2218 (2000).

[43] H. J. C. Berendsen, J. R. Grigera, and T. P. Straatsma, J. Phys. Chem. **91**, 6269 (1987).

[44] D. N. Bernardo, Y. Ding, K. Krogh-Jespersen, and R. M. Levy, J. Phys. Chem. **98**, 4180 (1994).

[45] A. J. Stone, A. Dullweber, O. Engkvist, E. Fraschini, M. P. Hodges, A. W. Meredith, P. L. A. Popelier, and D. J. Wales, *Orient: A Program for Studying Interactions Between Molecules, Version 4.4*, University of Cambridge, 2000, http://fandango.ch.cam.ac.uk/.

[46] B. M. Axilrod and E. Teller, J. Chem. Phys. **11**, 299 (1943).

[47] Y. Muto, Proc. Phys. Math. Soc. Japan **17**, 629 (1943).

[48] E. M. Mas, R. Bukowski, and K. Szalewicz, J. Chem. Phys. **118**, 4404 (2003).

[49] J. A. Alejandre, D. J. Tildesley, and G. A. Chapela, J. Chem. Phys. **102**, 4574 (1995).

[50] L. X. Dang and T.-M. Chang, J. Chem. Phys. **106**, 8149 (1997).

[51] F. Keutsch, J. Cruzan, and R. J. Saykally, chem. Rev. (in press) (unpublished).

[52] K. Kim, K. D. Jordon, and T. S. Zwier, J. Am. Chem. Soc. **115**, 11568 (1994).

[53] S. M. Kathman, G. K. Schenter, and B. C. Garrett, J. Chem. Phys. **111**, 4688 (1999).

[54] L. B. Braly, Ph.D. thesis, University of California, Berkeley, 1999.

[55] M. G. Brown, M. R. Viant, R. P. McLaughlin, C. J. Keoshian, E. Michael, J. D. Cruzan, and R. J. Saykally, J. Chem. Phys. **111**, 7789 (1999).

[56] S. Xantheas and T. H. Dunning, J. Chem. Phys. **99**, 8774 (1993).

Tables

	$(H_2O)_2$	
MODEL	$D_e(\mathrm{cm}^{-1})$	$D_0(\mathrm{cm}^{-1})$
MP2[a]	-1773	-910
ASP-NB[a]	-1641	-981
VRT(ASP-W)II	-1544	-1055
VRT(ASP-W)III	-1678	-1080
SAPT5s	-1699[b]	-1067[c]
PSPC	-3125	-901
SPC/E	-4499	-1664

Table 1: Well depths (D_e) and dissociation energies (D_0) of the dimer as described in the text. [a]Results from Gregory and Clary [28]. [b]Mas et al [6]. [c]Groenenboom et al [4].

$(H_2O)_2$	VRT(ASP-W)II	VRT(ASP-W)III	SAPT5s[a]	PSPC	SPC/E	Experiment[b]
A (GHz)	232.01	230.36	207.76	219.53	222.549	227.6
B (GHz)	6.01	5.99	$\frac{B+C}{2}$ =	6.16	6.752	$\frac{B+C}{2}$ =
C (GHz)	5.95	5.92	6.13	6.07	6.647	6.16

Table 2: Vibrationally averaged dimer rotational constants. [a]Groenenboom et al [4]. [b]Experimental results from [54], p. 133 and p.170.

$(H_2O)_3$	(uud)		(uuu)	
MODEL	D_e (cm^{-1})	D_0 (cm^{-1})	D_e (cm^{-1})	D_0 (cm^{-1})
MP2[a]	-5501	-3008	-5214	-2919
ASP-NB[a]	-5626	-3509	-5297	–
VRT(ASP-W)II	-5615	-3619	-5432	–
VRT(ASP-W)III	-5432	-3557	-5307	–
SAPT5s+3B	-5287[b]	-3610	-5090[b]	–
PSPC	–	-2601	–	–
SPC/E	–	-2279	–	–

Table 3: D_e and D_0 for the lowest two trimer potential minima. Results for both the (uud) and (uuu) structures are shown. The value of D_0 for (uuu) could not be calculated with local minima constraints (see text for discussion). [a]Gregory and Clary [28]. [b]Mas et al [7].

$(H_2O)_3$	VRT(ASP-W)II	VRT(ASP-W)III	SAPT5s+3B	PSPC	SPC/E	Expt.[a]
A (GHz)	7.04	6.84	6.87	6.74	6.614	6.646
B (GHz)	5.85	5.68	5.72	5.49	5.324	6.646
C (GHz)	3.24	3.15	3.16	3.05	2.973	3.513 (AF)

$(D_2O)_3$	VRT(ASP-W)III	ASP-NB	Experiment[a]
A (GHz)	5.942	6.886	5.796
B (GHz)	4.997	6.769	5.796
C (GHz)	3.167	3.534	AF

Table 4: Vibrationally averaged $(H_2O)_3$ and $(D_2O)_3$ rotational constants for (uud). [a]Experimental results are from [55]. The value of C could not be determined experimentally and hence was arbitrarily fixed(AF).

$(H_2O)_4$	(udud)	
Model	D_e (cm^{-1})	D_0 (cm^{-1})
MP2[a]	-10016	-6148
ASP-NB[a]	-10058	-6412
VRT(ASP-W)II	-10093	-6732
VRT(ASP-W)III	-10052	-6750
SAPT5s+NB(ASP)	–	-6338
PSPC	–	-4486
SPC/E (uudd)	–	-3981

$(H_2O)_4$	D_e (cm^{-1})			
Model	(uudd)	(uuud)	cage	C_S
MP2[a]	-9715	not a minimum	N/A	-7575
ASP-NB[a]	-9683	-9630	N/A	-8211
VRT(ASP-W)II	-9729	-9717	-8637	-7668
VRT(ASP-W)III	-9709	-9687	–	–

Table 5: D_e and D_0 for the (udud) tetramer structure, and D_e for the (uudd) and (uuud) structures. The VGS for SPC/E was found to be (uudd), as noted. [a]Gregory and Clary [28]. The cage results for ASP-NB and the MP2 calculations are marked as N/A because the cage structure collapsed to (udud) in both cases. The results for the cage and C_S tetramer of VRT(ASP-W) are left blank because corresponding stable local minima could not be found.

$(H_2O)_4$	VRT(ASP-W)II	VRT(ASP-W)III	SAPT5s+NB(ASP)	PSPC	SPC/E
A (GHz)	3.70	3.64	3.60	3.52	3.450
B (GHz)	3.17	3.11	2.99	2.88	2.817
C (GHz)	1.75	1.72	1.68	1.61	1.576

$(D_2O)_4$	VRT(ASP-W)III	ASP-NB	Experiment[a]
A (GHz)	3.183	3.063	3.080
B (GHz)	2.765	3.063	3.080
C (GHz)	1.536	1.583	AF

Table 6: Rotational constants for (udud) of the tetramer.

$(H_2O)_5$	Ground-state	
MODEL	$D_e(cm^{-1})$	$D_0(cm^{-1})$
MP2 (cyclic)	-13341	–
ASP-NB [cage(6)]	-13179	-8571
VRT(ASP-W)II (envelope)	-13264	-8907
VRT(ASP-W)III (cyclic)	-13399	-9081
SAPT5s+NB(ASP) (cyclic)	–	-8522
SAPT5s+NB(ASP-T) (cyclic)	–	-8734
PSPC (cyclic)	–	-6010
SPC/E (tetrahedron)	–	-9134

Table 7: D_e and D_0 for the $(H_2O)_5$ minimum energy structures. [a] D_0 for the MP2 surface was not calculated by Gregory and Clary [28].

$(H_2O)_5$	Envelope		Cyclic		Cage(6)
Model	D_e (cm^{-1})	D_0 (cm^{-1})	D_e (cm^{-1})	D_0 (cm^{-1})	D_e (cm^{-1})
MP2	-12572	–	-13341	–	-12308
ASP-NB	-13072	-8414	-13124	-8389	-13179
VRT(ASP-W)II	-13264	-8907	-13417	–	-12916
VRT(ASP-W)III	-13194	-8929	-13399	-9081	-12741

Table 8: D_e and D_0 for all investigated structures of the pentamer. RBDMC simulations with VRT(ASP-W)II and III constrained to the cage(6) minimum collapsed to their respective ground-state. Cage(7) structures could not be located on the VRT(ASP-W)II and III potential surfaces.

$(H_2O)_5$	VRT(ASP-W)II[a]	VRT(ASP-W)III	SAPT5s+NB(ASP)	SAPT5s+NB(ASP-T)	PSPC	SPC/E[b]
A (GHz)	2.389	2.280	2.05	2.05	1.995	3.321
B (GHz)	1.901	1.731	1.72	1.75	1.623	1.073
C (GHz)	1.668	1.074	0.98	0.98	0.920	0.919

$(D_2O)_5$	VRT(ASP-W)III	ASP-NB[a]	Experiment[b]
A (GHz)	1.832	1.739	1.750
B (GHz)	1.602	1.739	1.750
C (GHz)	0.894	0.849	AF

Table 9: Vibrationally averaged ground-state rotational constants for the pentamer. [a]Rotational constants of the envelope structure. [b]Rotational constant of the tetrahedral pentamer.

$(H_2O)_6$	Global minimum	
MODEL	D_e (cm^{-1})	D_0 (cm^{-1})
MP2 (prism)[a]	-16577	–
ASP-NB (cage)	-17545	-11536
VRT(ASP-W)II (prism)	-17601	-12042
VRT(ASP-W)III (cage)	-17478	-11814
SAPT5s+NB(ASP) (book)	–	-11095
SAPT5s+NB(ASP-T) (cage)	–	-10999
PSPC (book)	–	-7389
SPC/E (bird)	–	-12994

Table 10: D_e and D_0 for $(H_2O)_6$ minimum energy structures. Listed in parenthesis next to the name of each model is the different ground-state structure it predicts. [a] D_0 for the MP2 surface was not calculated by Gregory and Clary [28].

$(H_2O)_6$	prism		cage		cyclic	book
MODEL	D_e (cm^{-1})	D_0 (cm^{-1})	D_e (cm^{-1})	D_0 (cm^{-1})	D_e (cm^{-1})	D_e (cm^{-1})
MP2	-16137	–	-16088	–	-16577	-16439
ASP-NB	-17566	-11418	-17545	-11536	-16028	-16941
VRT(ASP-W)II	-17601	-12050	-17185	–	-16613	–
VRT(ASP-W)III	-17478	-11663	-17069	-11814	-16605	-16357

Table 11: D_e and D_0 for the prism, cage, and cyclic hexamer structures. The book for VRT(ASP-W)II was not investigated. [a]RBDMC simulations with VRT(ASP-W)II all collapsed to the prism. [b]RBDMC simulations of VRT(ASP-W)III for the cyclic and book collapsed to the cage. Hence, values of D_0 for these structures are not shown in the above table.

$(H_2O)_6$	VRT(ASP-W)II[a]	VRT(ASP-W)III[b]	SAPT5s +NB(ASP)[c]	SAPT5s +NB(ASP-T)[b]	PSPC[c]	SPC/E[d]	ASP-NB[b]	Experiment[a]
A (GHz)	1.678	2.107	1.83	2.08	1.789	1.581	2.136	2.164
B (GHz)	1.352	1.100	1.03	1.06	0.922	1.281	1.096	1.131
C (GHz)	1.266	1.025	0.74	0.94	0.673	1.053	1.043	1.069

Table 12: $(H_2O)_6$ vibrationally averaged rotational constants for ground-state structures. [a]Prism. [b]Cage. Experimental results are from [21]. [c] Book. [d]Bird.

a)

$(H_2O)_3$	ASP-NB	ASP-W	% change
(uud)	-5626	-5699	1.28
(uuu)	-5297	-5368	1.32

b)

$(H_2O)_4$	ASP-NB	ASP-W	% change
(udud)	-10058	-10083	0.25
(uudd)	-9683	-9715	0.33
(uuud)	-9630	-9666	0.37
C_S	-8211	-7310	12.33

c)

$(H_2O)_5$	ASP-NB	ASP-W	% change
Cage(6)	-13179	-12973	-1.59
Cyclic	-13124	-13119	-0.04
Envelope	-13072	-13152	0.61
Cage(7)	-12868	-12846	-0.16

d)

$(H_2O)_6$	ASP-NB	ASP-W	% change
Prism	-17566	-17649	0.47
Cage	-17545	-17276	-1.55
Book	-16941	–	–
Boat	-16235	-16393	0.96
Cyclic	-16028	-16072	0.31

Table 13: Effect of three-body dispersion on ES for the water trimer through hexamer. All values for D_e are in cm^{-1}, and the percentage of change is calculated relative to ASP-W.

ASP-W	D_0 (cm^{-1})	Structure	% change
$(H_2O)_3$	-3564	(uud)	-1.54
$(H_2O)_4$	-6593	(udud)	-2.75
$(H_2O)_5$	-8722	envelope	-3.66
$(H_2O)_6$	-11975	prism	-4.65

Table 14: Effects of 3-body dispersion on VGS. Percent change is calculated from ASP-NB, relative to ASP-W.

	ASP-W			
	$(D_2O)_3$	$(D_2O)_4$	$^a(D_2O)_5$	$^b(H_2O)_6$
A (GHz)	6.119	3.248	1.864	1.634
B (GHz)	5.147	2.818	1.634	1.374
C (GHz)	2.904	1.574	0.925	1.266

Table 15: Ground-state rotational constants for the trimer through hexamer. ^{a}Envelope structure. ^{b}Prism structure.

Figures

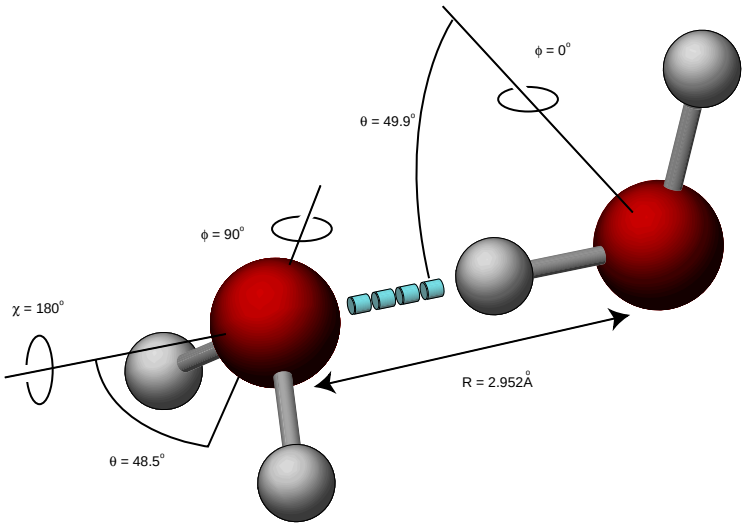

Figure 1: Equilibrium structure of the water dimer obtained from VRT(ASP-W)III.

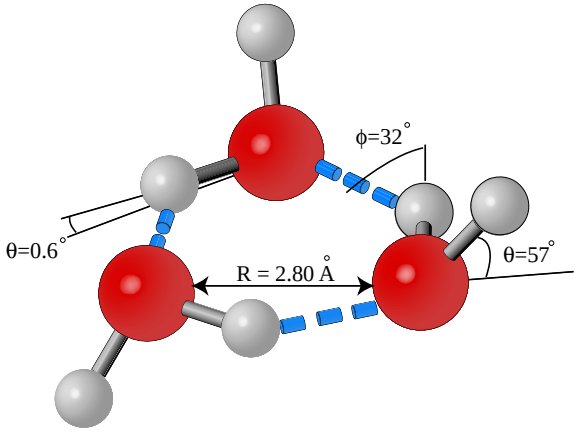

(a) (uud)

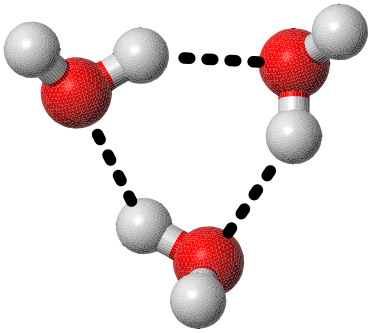

(b) (uuu)

Figure 2: $(H_2O)_3$ equilibrium structures from VRT(ASP-W)III. *Ab initio* equilibrium structural properties of the (uud) structure are given in [56].

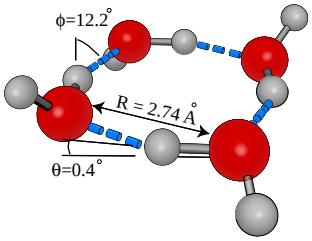

(a) (udud)

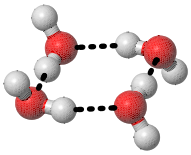

(b) (uudd)

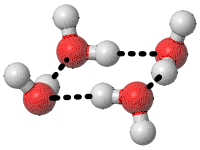

(c) (uuud)

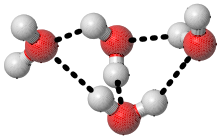

(d) C_s

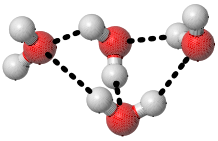

(e) Cage

Figure 3: Equilibrium structures for the water tetramer obtained from the original ASP-W. *Ab initio* equilibrium structural properties of the (udud) structure are shown (from Ref. [56]).

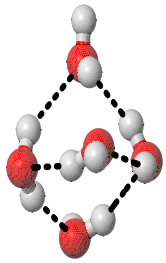

(a) Cage (6)

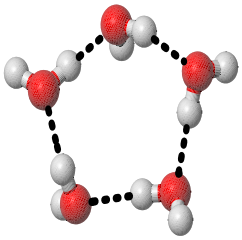

(b) Cyclic

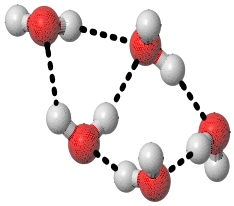

(c) Envelope

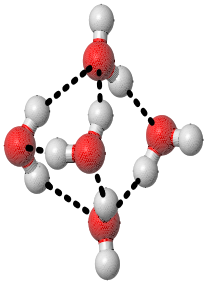

(d) Cage (7)

Figure 4: Equilibrium structures for the water pentamer, obtained from ASP-W.

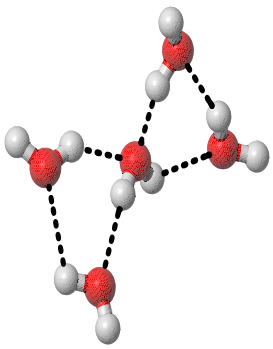

Figure 5: $(H_2O)_5$ VGS for SPC/E, an ice-like pentamer or tetrahedron.

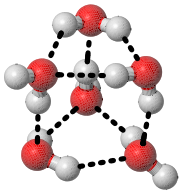

(a) prism

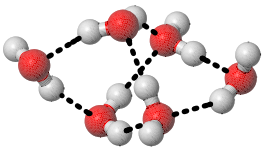

(b) Cage

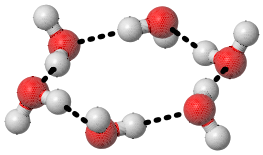

(c) Cyclic

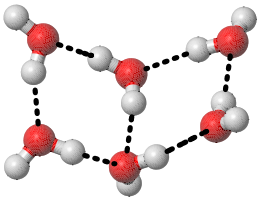

(d) Book

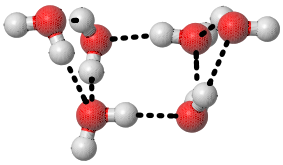

(e) Boat

Figure 6: The low energy structures of the hexamer investigated in this study. Results for the boat structure are not presented in this paper but the structure is included in this figure for the sake of completeness.

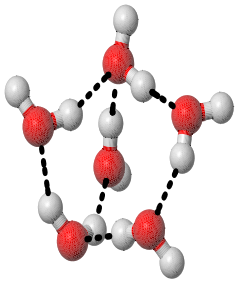

Figure 7: Vibrationally averaged ground-state D_0 structure for SPC/E, named the "bird" structure.

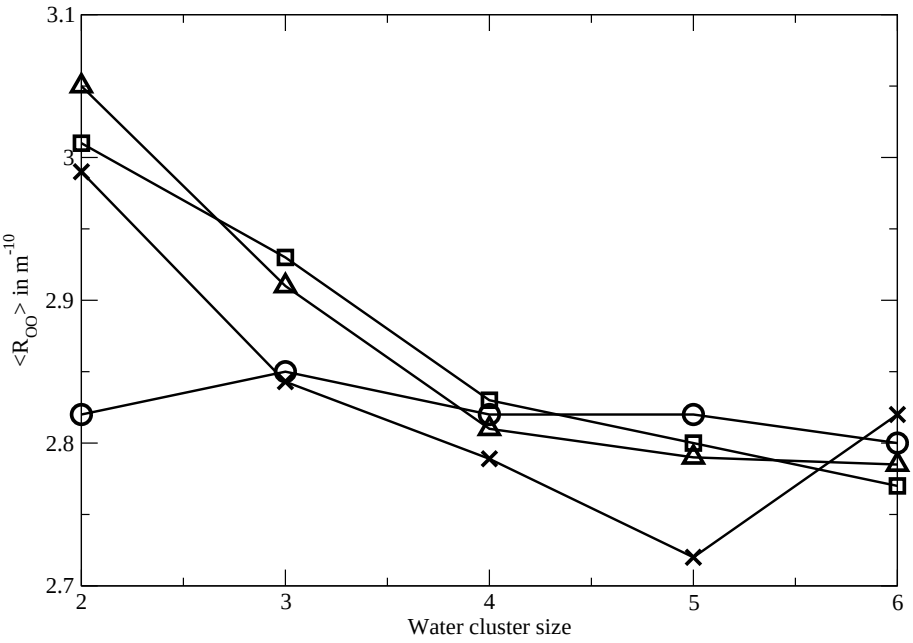

Figure 8: Vibrationally averaged ground-state $\langle R_{OO} \rangle$ [Å] values for several potentials compared with experiment. X's correspond to experimental results, open squares to VRT(ASP-W)III, open triangles to ASP-NB [28], and circles to SPC/E.